

1
2
3
4
5
6
7 pH and glucose dual-responsive injectable hydrogels
8
9
10
11 with insulin and fibroblasts as bioactive dressings
12
13
14
15
16 for diabetic wound healing
17
18
19

20
21 *Lingling Zhao^{1,3*}, Lijing Niu¹, Hongze Liang¹, Hui Tan^{2*}, Chaozong Liu³ and Feiyan Zhu⁴*
22

23
24 ¹Ningbo University, Faculty of Materials Science and Chemical Engineering, Ningbo, 315211,
25
26 China.
27

28
29 ²Shenzhen Second People's Hospital, Shenzhen Key Laboratory of Neurosurgery, Shenzhen,
30
31 518035, China.
32

33
34 ³University College London, Division of Surgery and Interventional Science, London, HA7 4LP,
35
36 UK.
37

38
39 ⁴Shenzhen Second People's Hospital, Shenzhen Key Laboratory of Tissue Engineering,
40
41 Shenzhen 518035, China.
42

43
44
45 **KEYWORDS**

46
47 Injectable hydrogel, wound dressing, drug delivery system, diabetic foot ulcers, wound
48
49 healing, pH responsive, glucose responsive
50

51
52
53 **ABSTRACT**
54
55
56
57
58
59
60

1
2
3 pH and glucose dual-responsive injectable hydrogels were prepared through the
4 crosslinking of Schiff's base and phenylboronate ester using phenylboronic modified chitosan,
5 polyvinyl alcohol and benzaldehyde-capped poly(ethylene glycol). Protein drugs and live cells
6 could be incorporated into the hydrogels during the *in situ* crosslinking, displaying sustained and
7 pH/glucose triggered drug release from the hydrogels, and cell viability and proliferation in the
8 three-dimensional hydrogel matrix as well. Hence, the hydrogels with insulin and fibroblasts
9 were considered as bioactive dressings for diabetic wound healing. A streptozotocin-induced
10 diabetic rat model was used to evaluate the efficacy of hydrogel dressings in wound repair. The
11 results revealed that the incorporation of insulin and L929 in the hydrogels could promote
12 neovascularization and collagen deposition, and enhance the wound healing process of diabetic
13 wounds. Thus, the drug- and cell-loaded hydrogels have promising potential in wound healing as
14 a medicated system for various therapeutic proteins and live cells.
15
16
17
18
19
20
21
22
23
24
25
26
27
28
29
30
31
32

33 **Introduction**

34
35
36
37 Diabetes mellitus is a complex metabolic disorder and has severely affected thousands of
38 people in the world.^{1,2} Diabetic foot ulcer (DFU) is a kind of lesion formed on the feet that
39 cannot proceed through the normal wound healing. It is a chronic, non-healing complication of
40 diabetes, leading to high hospital costs and even amputation.³⁻⁵ The medical treatment of DFU
41 remains a challenge. Historically, wound dressings were first considered to take a passive and
42 protective effect in the wound-healing process. The development of novel and efficient wound
43 dressings is very important for wound repair, and an ideal wound dressing should provide a
44 moist wound environment to the wound area, offer protection from secondary infections, remove
45 wound exudate and promote tissue regeneration.^{3,6,7} It is widely believed that DFU therapy
46
47
48
49
50
51
52
53
54
55
56
57
58
59
60

1
2
3 should actively promote wound healing by correcting the expression of biological factors that are
4 important in the healing process.⁸ The development of next-generation DFU therapies include
5 three technologies, topical drug treatment (e.g. insulin and growth factors), cellular therapies (e.g.
6 stem cells and fibroblasts) and scaffolds as well, and most current treatments employ one of
7 these approaches.⁹⁻¹² However, DFU is a complex clinical problem, and necessary combination
8 of technologies for diabetic foot ulcer therapy should be taken into account to address effectively
9 the complex underlying pathology and enable reliable DFU repair. Thus, wound dressings could
10 be considered as medicated systems, combining drug treatment, cellular therapy and scaffold for
11 DFU treatment.
12
13
14
15
16
17
18
19
20
21
22
23
24

25
26 Hydrogels have attracted increasing attentions in the past decades for biomedical
27 application,¹³⁻¹⁷ and the utility of hydrogels as wound dressing became focused in recent
28 years.^{18,19} Hydrogels contain a large amount of water due to their three-dimensional hydrophilic
29 polymeric networks, and hence provide a moist environment to the wound area, helping wounds
30 to heal faster.³ There are many reports on wound dressing with bioactive substances (protein
31 drugs, growth factors, live cells and so on) for diabetic wound healing,^{2,3,10,18} while very a few
32 works have considered the special physiological environment of diabetic ulcer area. High level
33 of glucose is an important factor for diabetes mellitus,^{4,20} and glucose control is likely of great
34 importance among metabolic factors.⁵ For the distinct physiological microenvironment between
35 diabetic ulcer and normal tissues, such as acidic pH and high levels of glucose,^{21,22} smart
36 hydrogels containing ‘sensor’ moieties which can respond to environmental pH and glucose
37 concentration,^{17,23,24} are ideal choices of wound dressings as medicated systems through the
38 smart drug delivery for diabetic wound healing. Moreover, hydrogels are ideal materials as
39 extracellular matrix (ECM) of various cells which would benefit the growth of skin tissue,^{25,26}
40
41
42
43
44
45
46
47
48
49
50
51
52
53
54
55
56
57
58
59
60

1
2
3 because live cells could secrete appropriate combinations and ratios of necessary factors for
4 enhanced tissue regeneration.⁹ In addition, injectable hydrogel is another attractive feature due to
5
6 its nonsurgical treatment to the patients for the purpose of mini-invasive medicine, especially for
7
8 the irregular trauma in the deeper parts.^{27,28} Thus, environmentally sensitive and injectable
9
10 hydrogels could provide a promising therapy for DFU treatment by combining these therapies
11
12 (smart drug delivery treatment, cell/tissue repair and extracellular matrix scaffold) to maximize
13
14 their DFU repair potential. Herein, in this work, considering the acidic pH and high glucose level
15
16 condition at diabetic ulcer area, smart hydrogels with pH and glucose responsibility are
17
18 developed to incorporate drug and cells as bioactive dressings for diabetic wound healing,
19
20 coupling drug treatment, cellular therapy and extracellular matrix scaffold into a whole.
21
22
23
24
25
26
27

28 In our previous work, pH and glucose sensitive injectable hydrogels were prepared through
29
30 the covalent crosslinking of imine bond and phenylboronate ester using phenylboronic modified
31
32 chitosan and oxidized dextran.²⁹ Drugs and cells can be incorporated into the hydrogels, allowing
33
34 responsive drug release and cell proliferation. In this work, phenylboronic modified chitosan
35
36 (CSPBA), polyvinyl alcohol (PVA) and benzaldehyde-capped poly (ethylene glycol) (OHC-
37
38 PEG-CHO) were employed as starting materials. Benzoic-imine bonds instead of imine bonds
39
40 were used to design the dually responsive hydrogels for benzoic-imine bond formed from
41
42 aliphatic amine and aromatic aldehyde group was more stable at physiological pH due to the π - π
43
44 conjugation.^{30,31} Studies showed that insulin could accelerate wound healing and skin repair in
45
46 diabetes by regulating some important factors in the skin's healing response, such as the function
47
48 of epidermal and dermal skin cells, vascular and immune cells,³²⁻³⁴ and fibroblasts loaded in the
49
50 hydrogel dressing could significantly improve the skin regeneration by favorable growth of
51
52 microvessels, hair follicles and faster formation of epidermis.¹⁹ Herein, insulin and fibroblasts
53
54
55
56
57
58
59
60

1
2
3 were selected as model drug and cells, to exploit insulin and fibroblasts dual-loaded smart
4 hydrogels as bioactive wound dressings for diabetic ulcer. The physicochemical properties of the
5 CSPBA/PVA/OHC-PEG-CHO hydrogels were characterized, and the diabetic ulcer repair
6 efficacy of the bioactive dressings was evaluated *in vivo* through SD diabetic wound rat model.
7
8
9
10
11
12

13 14 **Experimental Section**

15 16 17 **Materials**

18
19
20 CSPBA (the PBA content in CSPBA is 0.32) and benzaldehyde capped poly (ethylene
21 glycol) (OHC-PEG-CHO) (MW~2000 Da) were synthesized according to our previous work.^{29,35}
22
23 Polyvinyl alcohol (PVA) (MW~4000 Da) and bovine insulin were purchased from Sigma
24
25 Aldrich (St. Louis, US). All the reagents were used as received without further purification.
26
27
28
29
30

31 **Preparation of CSPBA/PVA/OHC-PEG-CHO hydrogels**

32
33
34 CSPBA and OHC-PEO-CHO solutions were prepared by dissolving the desired amount of
35 polymer in distilled and deionized water. PVA solution was obtained by dissolving the desired
36 amount of polymer in distilled and deionized water at 90 °C and then cooled down to room
37 temperature. The pH of the solution was adjusted to 7.4 using 2 M HCl/NaOH. As a typical
38 hydrogel preparation, 0.25 mL of PVA solution was added to 0.25 mL of OHC-PEO-CHO
39 solution to get a mixed solution, and then 0.5 mL of CSPBA solution was added. The gelation
40 occurred within ~10-20 s of stirring.
41
42
43
44
45
46
47
48
49
50
51

52 **Characterization of CSPBA/PVA/OHC-PEG-CHO hydrogels**

53 54 55 **Rheological analysis**

1
2
3 The rheological behavior of the hydrogels was performed on a rheometer with a 20 mm-
4 diameter parallel plate (Rheo Stress I, KAAKE) at 37 ± 0.1 °C. Both G' (elastic moduli) and G''
5 (loss moduli) of the CSPBA/PVA/OHC-PEO-CHO aqueous at different pH and polymer content
6 were tested to characterize the viscoelasticity. The desired amount of CSPBA, PVA and OHC-
7 PEO-CHO were dissolved in water to form sample solutions respectively, and the pH of the
8 solution was adjusted to the required value using 2 M HCl/NaOH. The solutions were firstly
9 mixed under vigorous stirring for 10 s to form a mixture, and then the mixture was quickly
10 poured onto the plate. A gap of 1 mm and a frequency of 1 rad/s were selected in the
11 measurement. To ensuring a linear viscoelastic region, strain amplitude of 2% was used in the
12 time sweeping tests. The frequency sweep was performed over the frequency range from 0.1 to
13 100 rad/s at a strain of 2%. Strain sweep analyses were carried out with pre-made hydrogels, G'
14 and G'' of the hydrogels were monitored under continuous strain sweep with alternate small
15 oscillation force ($\gamma = 2\%$ strain) and a large one ($\gamma = 200\%$ strain).
16
17
18
19
20
21
22
23
24
25
26
27
28
29
30
31
32
33
34

35 **Scanning Electron Microscopy (SEM)**

36
37
38 Hydrogels prepared with different polymer composition were freeze-dried, and the cross-
39 section morphology of the hydrogels was performed on a Hitachi S-4800 scanning electron
40 microscope.
41
42
43
44
45

46 **Drug loading and Release**

47
48
49 CSPBA, PVA and OHC-PEO-CHO solutions were prepared by dissolving the desired
50 amount of polymer in water respectively, and the pH of the solution was adjusted to 7.4 using 2
51 M HCl/NaOH. Insulin was supplemented in the CSPBA solution under stirring to obtain a
52 CSPBA/insulin solution. Equivalent volume (0.25 mL) of PVA and OHC-PEO-CHO solution
53
54
55
56
57
58
59
60

1
2
3 were firstly mixed and then added into the CSPBA/insulin solution (0.5 mL). The mixed solution
4
5 was stirred vigorously to enable the hydrogel formation. After 30 min of incubation to ensure
6
7 fully crosslinking of the hydrogels, the insulin-loaded hydrogels were immersed into 10 mL of
8
9 media (0.01 M PBS containing the desired amount of glucose at different pH) in the vials at
10
11 37 °C. At desired time point, 2 mL of the release solution was collected from the vial and 2 mL
12
13 of fresh PBS was added after each sampling to keep the volume of the total medium in the vial
14
15 constant. The released drug was determined by RP-HPLC with a UV detector set at 227 nm. 20
16
17 μL of sample was injected into YMC-Pack Protein-RP column (150 mm \times 4.6 mm, 5.0 μm ,
18
19 Agilent Corp., USA) and eluted with the mobile phase consisted of acetonitrile/methanol (32/68,
20
21 v/v) containing 0.15% TFA at a flow rate of 1 mL/min. The mean value of three repeated tests
22
23 was used to plot the release results.
24
25
26
27
28
29

30 ***In vitro* Cell Culture in Hydrogels**

31
32
33 L929 cells were cultured using the complete DMEM medium at 37 °C in 5% CO₂, 95%
34
35 humidified atmosphere in a cell incubator and were subcultured every 48 h. Before testing, the
36
37 cells were harvested by trypsinization and re-dispersed in PBS at a desired cells density for use.
38
39
40
41

42 CSPBA, PVA and OHC-PEO-CHO were dissolved in DMEM medium at the required
43
44 concentration respectively. The solution was irradiated with UV light for 15 min for sterilization.
45
46 CSPBA solution (100 μL) was firstly mixed with the cells suspension (200 μL) in a 96-well.
47
48 Then a mixture of PVA/OHC-PEO-CHO solution (100 μL , v/v, 1/1) was added and the hydrogel
49
50 containing 1.2×10^6 cells/mL was formed under uniformly stirring. The cells-incorporated
51
52 hydrogels were then transferred into a 24-well plate carefully and cultured in a cell incubator. 1
53
54
55
56
57
58
59
60

1
2
3 mL of DMEM medium (with or without glucose) was added to each well of the 24-well plate
4
5 and replaced every day.
6
7

8
9 The viability of L929 cells in the hydrogels was determined using acridine orange (AO)
10 staining. The hydrogels were cut into thin slices and rinsed twice with PBS after 1 or 3 days'
11 cultivation. The hydrogel slices were stained using 5 μ L of AO dissolved in PBS (0.1 mg/mL)
12 for 30 s, and then the cells viability were performed using confocal laser scanning microscope
13 (Leica TCSsp2, Germany) at an excitation wavelength of 488 nm and an emission wavelength of
14 515 nm. The proliferation analysis of cells in the hydrogel was tested using cell counting assay
15 (CCK). The cells-incorporated hydrogels in 24-well plates were rinsed twice with PBS after 1 or
16 3 days' cultivation, and then PBS (200 μ L) and CCK solution (10 μ L) was added to each well.
17 The mixture was incubated at 37°C and 5% CO₂ for 2 h with gentle shaking, and then a 150 μ L
18 aliquot of the solution in each well was transferred into a 96-well plate individually. The
19 absorbance at 450 nm was tested using an OPTI Max microplate reader.
20
21
22
23
24
25
26
27
28
29
30
31
32
33
34
35

36 ***In vivo* diabetic wound healing study**

37 38 39 **Preparation of Streptozotocin (STZ)-induced diabetic animal model**

40
41
42
43 Type 1 diabetes SD rats were induced by intraperitoneal injections of streptozotocin (STZ,
44 Sigma-Aldrich) dissolved in citrate buffer (0.05 M, pH 4.5) at a dosage of 100 mg/kg body
45 weight. Blood glucose levels were monitored by a glucose meter (Johnson, China) one week
46 after induction of diabetes. A hyperglycemic phenotype was confirmed when blood glucose
47 levels were over 300 mg/dL in the animals. The animal experiments were performed according
48 to the guidelines in the Department of Medicine, Ningbo University, China.
49
50
51
52
53
54
55
56
57
58
59
60

Diabetic wound treatment with hydrogel dressings

STZ-induced diabetic SD rats (male, 9-week-old) were randomly divided into four groups (n=7). Under anesthetization, the back of each rat was shaved. Then a full-thickness skin wound (10 mm in diameter) was created on the back of each rat after sterilization using 70% ethanol. The wounds were immediately treated with 0.5 mL of PBS (group 1, control), 0.2 mL of CSPBA/PVA/OHC-PEO-CHO hydrogels consisted of 1.2 wt% CSPBA, 0.6 wt% OHC-PEG-CHO and 0.6 wt% PVA (group 2), insulin-loaded CSPBA/PVA/OHC-PEO-CHO hydrogels consisted of 1.2 wt% CSPBA, 0.6 wt% OHC-PEG-CHO, 0.6 wt% PVA and 0.3 wt% insulin (group 3), CSPBA/PVA/OHC-PEO-CHO hydrogels encapsulating both insulin and L929 cells (1.2 wt% CSPBA, 0.6 wt% OHC-PEG-CHO, 0.6 wt% PVA, 0.3 wt% insulin and 1.2×10^6 cells/mL, group 4), respectively. The administration of PBS was achieved by dropping it onto the wound area, and the hydrogel formulations were loaded by plastering to cover the entire defect. Within the experimental time, the wound areas were recorded using a camera and the blood glucose was measured at desired time points. On predetermined time points, two rats in each group were sacrificed for histopathological or immunohistochemical analysis.

Wound closure measurement

The wound area of each animal was photographed at desired time points using a digital camera. Image J software was used to measure the wound area, and the wound size and wound closure degree were evaluated as well. The wound area was calculated using the following equation: $Wound\ area\ (\%) = (A_0 - A_t)/A_0 \times 100$, where A_0 is the wound area on the surgery day and A_t is the wound area at the indicated time point. The definition of wound repair completion was referred when the wound area was equivalent to the area at time point zero.

Measurement of blood glucose

For all animals, blood obtained from the tail vein at desired time point was tested using a blood glucose test meter and the blood glucose level was analyzed.

Histopathological and immunohistochemical analysis

The back skin around the wound site of the sacrificed rats was removed and fixed in 10% formaldehyde solution. The isolated tissues were embedded in paraffin and sectioned at a thickness of 4 μm . The sections were stained with hematoxylin/eosin (H&E), anti-CD31 antibody and Masson's trichrome (MT) to evaluate general aspects of the inflammatory infiltrate, neovascularization and collagen formation, under the standard procedures.

Statistics analysis

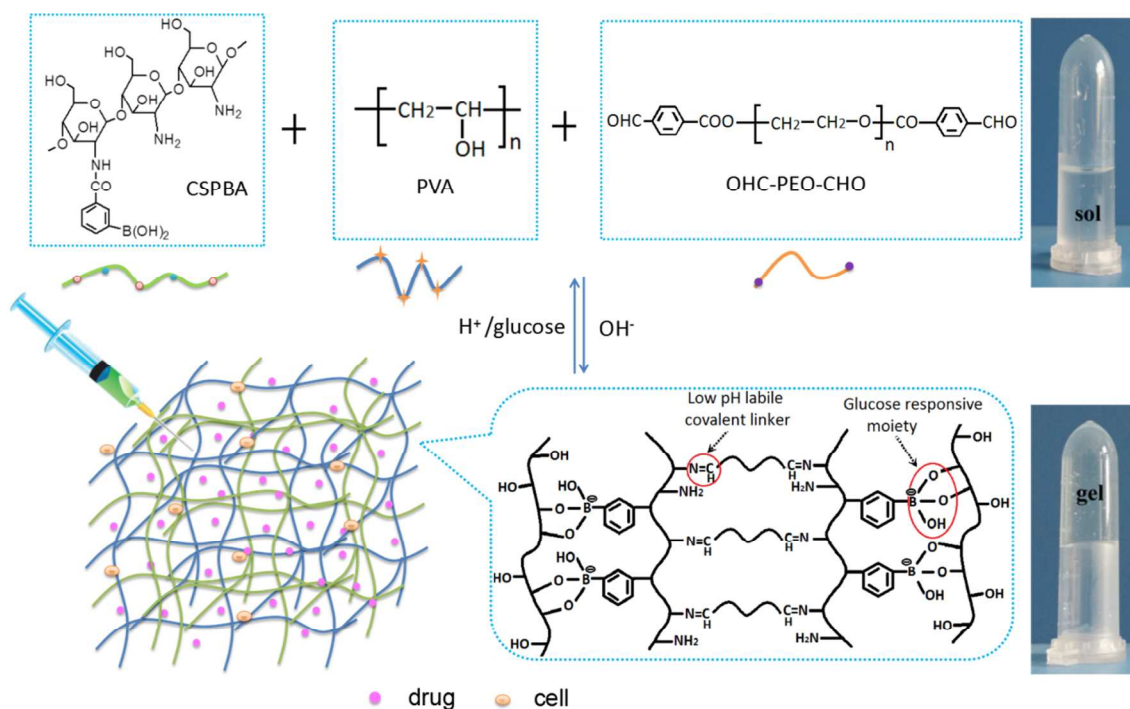
Statistical significance was assessed using one-way ANOVA method. The difference was considered to be statistically significant if the p value was less than 0.05.

Results and discussion

Hydrogel Formation

CSPBA/PVA/OHC-PEO-CHO hydrogels were formed through the crosslinking of pH responsive benzoic-imine (Schiff's base) and glucose responsive phenylboronate ester and allowed no inclusion of extraneous reagents except water. The friendly and *in situ* crosslinking process enabled the encapsulation of drug and cells into the hydrogel simultaneously. The formation of hydrogel was illustrated in Scheme 1. Sol-to-gel of the polymer solution can be observed by mixing the CSPBA, PVA and OHC-PEO-CHO solutions at pH 7.4 and the formed

hydrogel can transform to solution again by adding a tiny amount of HCl. The reversible sol-to-gel and gel-to-sol transitions can be repeated several times by adding a tiny amount of NaOH or HCl, indicating the repeatability of pH responsiveness. The gel-to-sol transition can also be observed by adding a tiny amount of glucose solution, showing the glucose responsiveness of the hydrogel. SEM images demonstrated that the lyophilized hydrogels were highly porous and had an interconnected polymer network due to the formation of ice crystal, which was in accordance with other reports.²⁹ The pore of the network became larger with lower crosslink density, as shown in Figure 1.



Scheme 1. Illustrative formation of the CSPBA/PVA/OHC-PEO-CHO hydrogel.

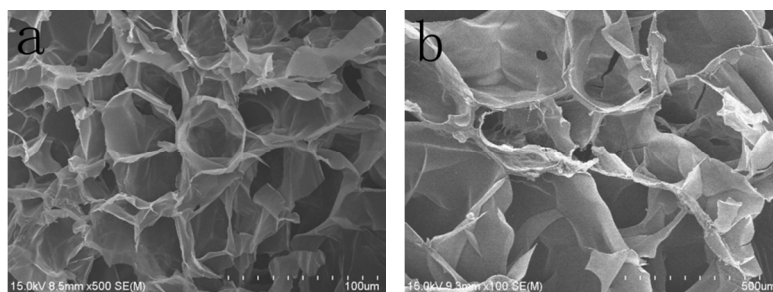


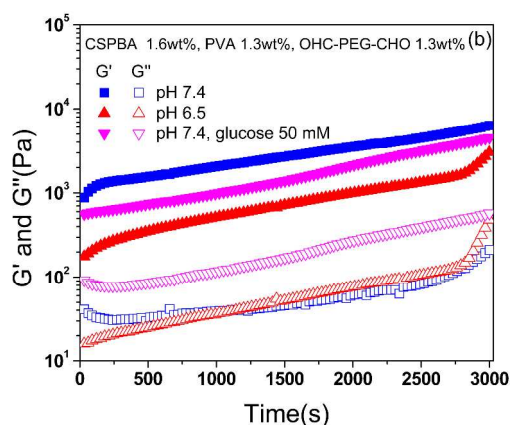
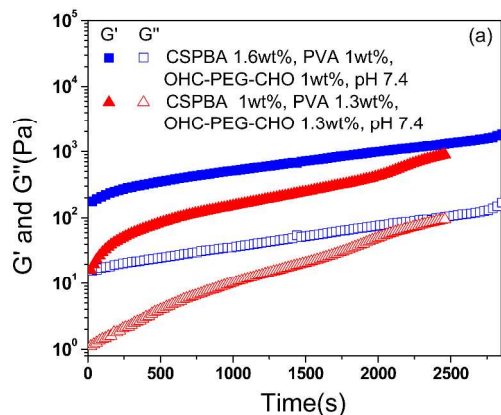
Figure 1. SEM images of CSPBA/PVA/OHC-PEO-CHO hydrogels formed at pH 7.4, consisting of 1.6 wt% CSPBA, 1wt% PVA and 1wt% OHC-PEO-CHO (a), and 1.6 wt% CSPBA, 0.5 wt% PVA and 0.5 wt% OHC-PEO-CHO (b).

Characterization of CSPBA/PVA/OHC-PEO-CHO hydrogels

The gelation behavior of the system and the dependence of the moduli of the hydrogels on the polymer content and environmental parameters (e.g. pH and glucose concentration) were demonstrated by rheological analysis. As plotted in Figure 2a and 2b, the G' surpassed G'' immediately after the addition of the PVA/OHC-PEO-CHO to CSPBA solution due to the quick formation of the hydrogel. This could provide the hydrogel formation from diffusion of the polymer solution to the surrounding tissues when it was injected into the body.³⁶ For the mixing process was slow on a parallel plate with a diameter of 20 mm, the G' value kept increasing due to the crosslinking reaction during the test process.²⁴ The moduli of hydrogels were also found to have a remarkable dependence on the polymer content, as shown in Figure 2a. The storage modulus G' of the hydrogel could reach to ~ 1 kPa at 1 wt% of CSPBA, 1.3 wt% of PVA and OHC-PEO-CHO. And the G' modulus was remarkably increased ($>5k$) with the increase of CSPBA concentration when the overall polymer concentration was kept constant in the hydrogel. For example, hydrogel consisted of 1.6 wt% of CSPBA, 1 wt% of OHC-PEO-CHO and 1 wt% of PVA in Figure 2a. In addition, the hydrogel formation was disparity when there was a small

1
2
3
4
5
6
7
8
9
10
11
12
13
14
15
16
17
18
19
20
21
22
23
24
25
26
27
28
29
30
31
32
33
34
35
36
37
38
39
40
41
42
43
44
45
46
47
48
49
50
51
52
53
54
55
56
57
58
59
60

change in the environmental parameters. As shown in Figure 2b, decreasing the pH from 7.4 to 6.8 could result in a modulus reduction and slowed gelation process of the hydrogel. Increasing the glucose concentration in the medium (50 mM) could also reduce the modulus of hydrogel remarkably when the pH was kept constant (Figure 2b). Thus the gelation process and hydrogel strength were adjustable by controlling the polymer composition and pH value, which was favorable for *in vivo* injection. However, once the hydrogels were stably formed, the G' was independent of the shear frequency from 0.1 to 100 rad/s because of the chemical crosslinking, i.e. the Schiff's base and phenylboronate ester, indicating that the gel was robust,³¹ as shown in Figure 2c. The rheological property of the hydrogels was in agreement with our previous work.²⁹



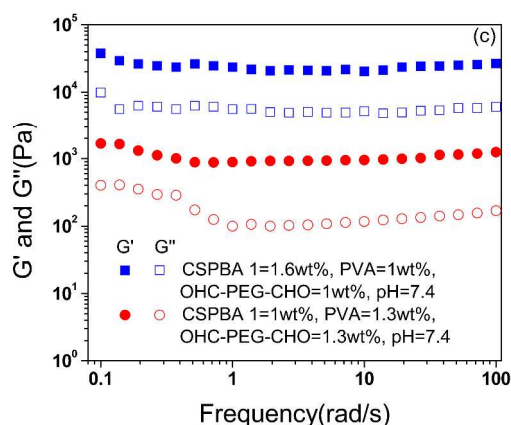
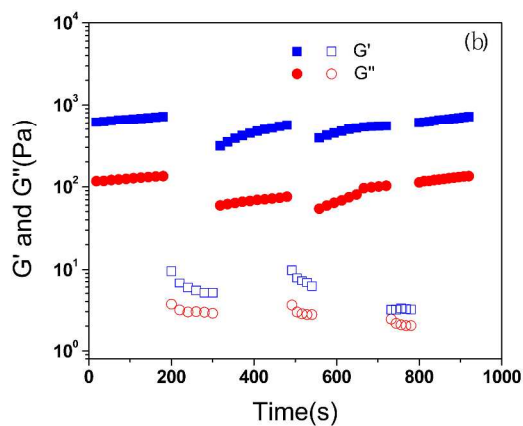
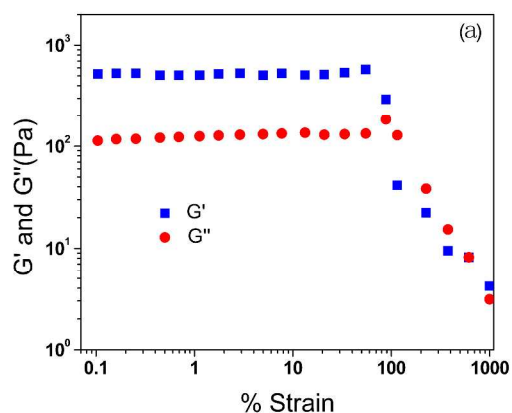


Figure 2. Time dependence (a, b) and frequency dependence (c) of elastic modulus (G' , solid symbols) and loss modulus (G'' , open symbols) of CSPBA/PVA/OHC-PEO-CHO mixtures at 37 °C with different polymer composition, glucose concentration and pH.

Since the hydrogel network is covalently cross-linked by dynamic Schiff's base and phenylboronate ester, it is expected to be injectable. Strain amplitude sweep was operated to demonstrate the elastic response of the hydrogel (CSPBA 1 wt%, PVA 1.3 wt% and OHC-PEO-CHO 1.3 wt%) with strain. The elastic modulus (G') decreased rapidly above the critical strain region ($\gamma=100\%$), as shown in Figure 3a, suggesting the collapse of the hydrogel network. Herein the hydrogel was performed on a large amplitude oscillatory strain of 200%, resulting in a decrease of G' from ~ 800 to ~ 10 Pa and $\tan \delta$ (G''/G') value at about 0.4 to 0.6 (Figure 3b). This means that the hydrogel has a loose network in large oscillatory force. It is noted that the G' recovered to the initial value quickly when the amplitude was decreased to a small strain of 2%, and the $\tan \delta$ (G''/G') value was about 0.11 to 0.18 (Figure 3b). This means that the inner network was quickly recovered and the hydrogel returned to the original state.³⁷

1
2
3
4
5
6
7
8
9
10
11
12
13
14
15
16
17
18
19
20
21
22
23
24
25
26
27
28
29
30
31
32
33
34
35
36
37
38
39
40
41
42
43
44
45
46
47
48
49
50
51
52
53
54
55
56
57
58
59
60

In vitro adhesive-healing test of the hydrogel was performed to further demonstrate the dynamic covalent cross-link in a macroscopic view. One piece of the hydrogel (CSPBA 1.6 wt%, PVA 1wt% and OHC-PEO-CHO 1 wt%, red hydrogel was obtained by adding a tiny amount of DOX for easy observation) was cut into two small pieces (Figure 3c), then the two pieces were placed closely together along the cut section in a container saturated with moisture in air. After incubation at room temperature for 30 min without any external stimulus, the two pieces of hydrogels merged together. As shown in Figure 3d, the merged hydrogel could be lifted up vertically by clamping at one side of the hydrogel using a tweezer without breaking into two pieces.



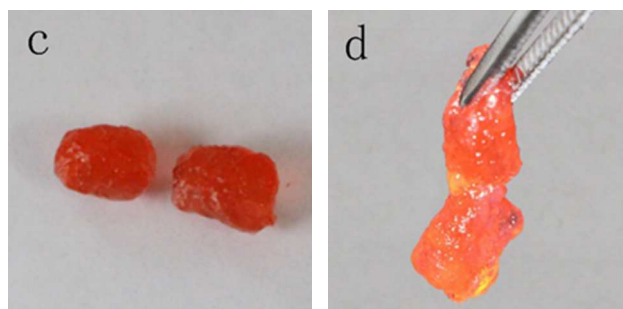


Figure 3. Rheology analyses of the dynamic and covalent crosslinked hydrogels. The dependence of elastic moduli (G') and loss moduli (G'') on strain amplitude (a); G' and G'' from continuous strain sweep with alternate small oscillation force ($\gamma=2\%$ strain, solid dots) and large oscillation force ($\gamma=200\%$, hollow dots) (b). The frequency was 1.0 Hz. Photos were taken during the adhesive-healing process of the hydrogel at 0 min (c) and 30 min (d).

***In Vitro* Drug Release**

Insulin is the most popular drug used in blood glucose control for diabetes mellitus. Herein, bovine insulin was adopted as a model drug and was encapsulated into CSPBA/PVA/OHC-PEO-CHO hydrogels at pH 7.4. Sustained and triggered drug release from the hydrogels could be observed (Figure 4). Decreasing the media pH or increasing the glucose level in the medium resulted in the accelerated insulin release from the hydrogels due to the swollen or hydrolysis of the hydrogel matrix, because the Schiff's base is labile at acidic pH,³¹ and phenylboronic group preferred to combine with glucose than hydroxyl group of PVA in the presence of glucose.²⁰ As shown in Figure 4a, at a release time of 34 h, the cumulative release of insulin was 9% at pH 7.4, and the value increased to 33 and 43% at pH 6.5 and pH 7.4 containing 3 mg/mL of glucose respectively. The drug release can be described using the followed formula: $M_t/M_\infty=kt^n$, where M_t/M_∞ is the fraction of drug released at time t varied from 0 to 1, and n is the diffusion related

1
2
3 component.^{29,38} The diffusion component n can be obtained by fitting the cumulative drug
4 release curve using Origin software and the calculated n values based on Figure 4a are 0.39, 0.32
5 and 0.33 at pH 7.4, pH 6.5 and pH 7.4 containing 3 mg/mL of glucose, respectively, indicating a
6 diffusion-controlled mechanism. This means that the insulin molecules diffuse mainly through
7 the swollen hydrogel matrix. Decreasing of CSPBA concentration and crosslinker content led to
8 the increase of insulin cumulative release from 9% (Figure 4a) to 39% (Figure 4b) at pH 7.4 after
9 releasing for 34 h. Similarly, decreasing the media pH or increasing the glucose level led to the
10 accelerated release of insulin from hydrogels. As shown in Figure 4b, the value increased from
11 39% at pH 7.4 to 80% and 50% at pH 6.5 and pH 7.4 containing 3 mg/mL of glucose at 34 h,
12 respectively. The calculated n values based on Figure 4b are 0.44, 0.62, and 0.57 at pH 7.4, pH
13 6.5 and pH 7.4 containing 3 mg/mL of glucose, respectively. This followed Fickian diffusion
14 mechanism under physiological condition attributed to the hydrophilicity of the drug. While the
15 kinetics deviated from the Fickian mechanism and followed non-Fickian behavior at acidic pH
16 and high level of glucose, indicating the diffusion of insulin molecules through the swollen
17 hydrogel matrix and the hydrolysis of hydrogels as well.^{29,38} The pH and glucose triggered drug
18 release indicates that the hydrogels should be positive for the application of the system in DFU
19 treatment due to the acidic pH and high glucose level in diabetes ulcer area.
20
21
22
23
24
25
26
27
28
29
30
31
32
33
34
35
36
37
38
39
40
41
42
43
44
45
46
47
48
49
50
51
52
53
54
55
56
57
58
59
60

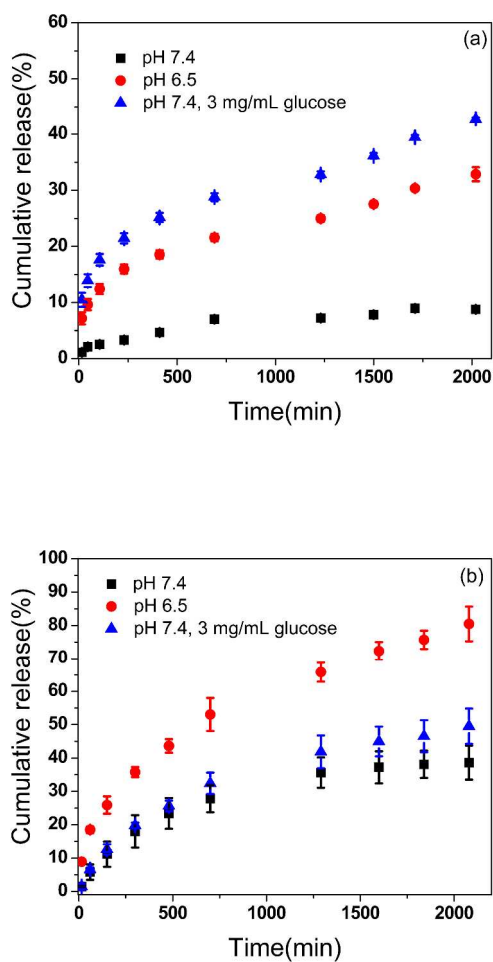
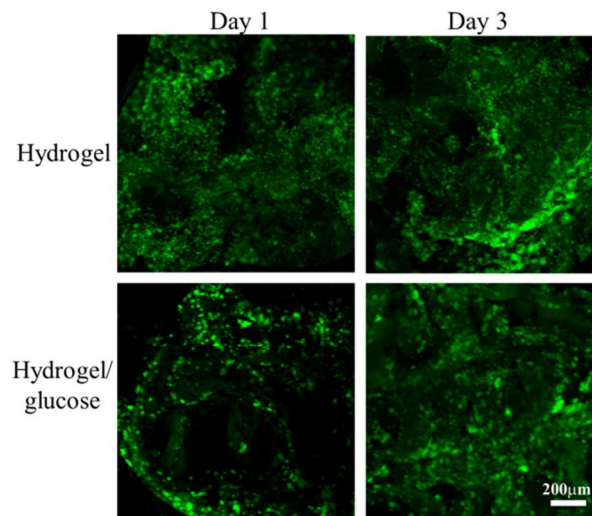


Figure 4. Cumulative drug release from the insulin incorporated hydrogels immersed in 10 mL of media with different pH and glucose concentration. (a) CSPBA 1.75 wt %, PVA 1 wt % and OHC-PEO-CHO 1wt %, (b) CSPBA 1.5 wt %, PVA 0.75wt % and OHC-PEO-CHO 0.75 wt %. The insulin loaded in each hydrogel was equivalent and was 3 mg/mL.

Cell Viability and Proliferation

Cell viability and proliferation were examined through three-dimensional cell cultivation in the hydrogel in order to demonstrate the biocompatibility and potential usage of hydrogels in drug/cell therapy. L929 fibroblasts were seeded and cultured in the hydrogels, and AO staining

1
2
3 showed uniform green fluorescence in both hydrogels with or without glucose on day 3, as
4 shown in Figure 5, displaying good viability of the cells cultivated in the hydrogels matrix.
5
6 Furthermore, the cell proliferation tested by CCK assay showed that L929 fibroblasts grew faster
7
8 in the hydrogels with lower cross-linkage density and polymer concentration. As shown in
9
10 Figure 6, the cell population in hydrogel-II (hydrogel with low polymer concentration and cross-
11
12 linkage density) was 1.8 times at day 3 compared with day 1. While the cells encapsulated in
13
14 Hydrogel-I (hydrogel with high polymer concentration and cross-linkage density) had no
15
16 significant proliferation at day 3. This may be because that the better swelling property and
17
18 looser network structure of the hydrogel with lower polymer concentration and cross-linkage
19
20 density were favorable to the interchange of substances and cell spreading, leading to an
21
22 accelerated proliferation of the cells. It is interesting to note that accelerated proliferation of the
23
24 cells was also observed when a small amount of glucose (3 mg/mL) was added into the culture
25
26 medium, and the number of cells in hydrogel-II with glucose medium was 2.2 times at day 3
27
28 compared with day 1 (Figure 6). The cell proliferation in the hydrogel matrix at high glucose
29
30 concentration and pH/glucose-responsive insulin release could endow the hydrogel system with
31
32 potential application in DFU treatment from both cell/tissue repair and drug therapy aspects.
33
34
35
36
37
38
39
40
41
42
43
44
45
46
47
48
49
50
51
52
53
54
55
56
57
58
59
60



22
23
24
25
26
27
28
29
30
31

Figure 5. CLSM images of L929 fibroblasts cultivated in the CSPBA/PVA/OHC-PEG-CHO hydrogels (CSPBA 1 wt%, OHC-PEG-CHO 0.5 wt%, PVA 0.5 wt%) for one day and three days. The concentration of glucose in the medium was 3 mg/mL. Scale bar: 200 μm.

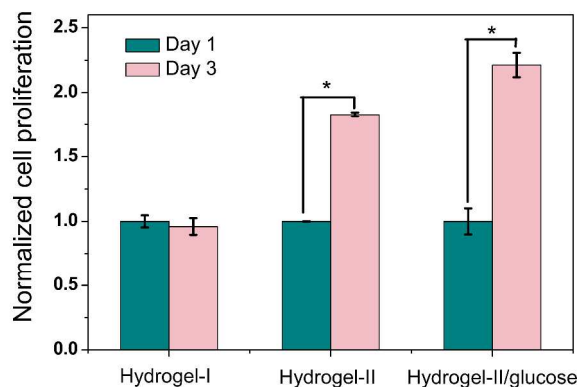


Figure 6. Population of cells cultivated in the CSPBA/PVA/OHC-PEO-CHO hydrogels for one day and three days ($*p < 0.05$). Cell population was normalized against the population on day 1. The polymer composition for Hydrogel-I was CSPBA 1.5 wt %, PVA 1wt % and OHC-PEO-CHO 1wt %, and for Hydrogel-II was CSPBA 1 wt%, OHC-PEO-CHO 0.5 wt%, PVA 0.5 wt%. The concentration of glucose in the medium was 3 mg/mL.

Effect of hydrogel dressings on the blood glucose in STZ-induced diabetic rats

A STZ-induced diabetic rat model was used to evaluate the effect of the drug and cells dual-loaded hydrogels in diabetic wound repair. Blood glucose levels in normal SD rats were 89.5 ± 6 mg/dL and elevated into a significantly high level of 325 ± 46 mg/dL in SD rats receiving STZ after 1 wk. Thereafter, wounds were created on the back of STZ-induced diabetic rats, then neat hydrogel, insulin and insulin/L929 loaded hydrogels were treated on the wound areas respectively, with the administration of PBS as a control. Blood glucose was monitored during the experimental period. The results showed that the blood glucose levels in the control group elevated to 609 ± 12 mg/dL within 6 days after wounding and then slightly dropped to 474 ± 76 mg/dL in the next 12 days (Figure 7). The blood glucose levels in the other three groups received hydrogel dressing treatment were suppressed in a certain level, which was much lower than that of the control group, while the blood glucose levels were still above 300 mg/dL except insulin/L929 loaded hydrogel group (Figure 7). For the hydrogel group, the blood glucose levels kept relatively steady without significant elevation within the first 10 days after wound treatment, possibly due to the blood-glucose-lowering effect of chitosan,^{39,40} but subsequently, the blood glucose levels increased again in the next 8 days. The blood glucose levels in insulin-loaded hydrogel group kept stable during the experimental period, which was significantly lower than that of the control group. While for the insulin/L929 loaded hydrogel group, the blood glucose levels dropped to below 300 mg/dL in the last 8 days. The relatively lower levels of blood glucose in insulin and insulin/L929 loaded hydrogels groups were possibly due to the sustained release of insulin from the hydrogels and the blood glucose management of chitosan. Diabetes has been shown to impair immune function and impede wound healing, as excessive glucose deposition in blood results in the peripheral neuropathy, which is critical to survival and recovery

from major wound injury.⁴¹ Hence the management of blood glucose of the hydrogel dressings is favorable for wound healing in diabetes.

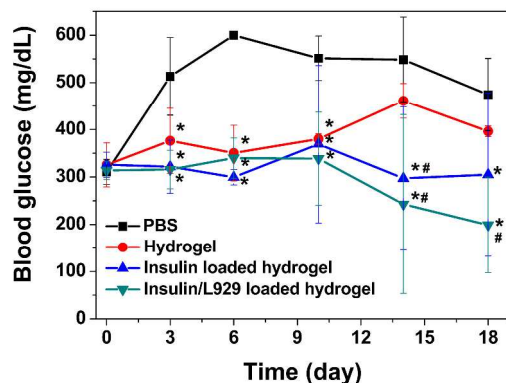


Figure 7. Changes in blood glucose in each diabetic rats group at varied time points. * $p < 0.05$ compared with PBS control group; # $p < 0.05$ compared with hydrogel group.

Effect of hydrogel dressings on wound healing in STZ-induced diabetic rats

To evaluate the wound healing capacity of the hydrogel dressings on diabetic skin wounds during the wound-repair process, images of the wound on the animals were taken at different time intervals, and wound areas and wound closure rate were calculated as well. As shown in Figure 8a, shrinkage of wound area was clearly seen for all groups with the growth of new epidermis extending to the center and recovering the whole lesion after 18 days post treatment. The wound closure rate was quantified and the results indicated that the groups treated with neat hydrogel, insulin and insulin/L929 loaded hydrogels displayed improved wound repair of the diabetic wounds after administration, compared with the control group (PBS). Specifically, the control group showed wound closure of $46 \pm 11\%$ of the initial wound area at day 6, and the diabetic skin wounds dealt with neat hydrogels revealed enhanced recovery potential with wound

1
2
3 closure of $60 \pm 7\%$ at day 6, as shown in Figure 8b. The facilitated healing process may be
4
5 contributed to the moist environment in the wound areas provided by the hydrogel. A similar
6
7 healing level of wound closure as the neat hydrogel group was observed in insulin-loaded
8
9 hydrogel group at day 6, and the wound closure was $63 \pm 4\%$. Interestingly, the wound closure in
10
11 insulin/L929 hydrogel group was significantly increased at day 6 ($70 \pm 11\%$), and the wound
12
13 area reached $92 \pm 8\%$ of closure at day 12, which was significantly enhanced compared with the
14
15 control and neat hydrogel groups. Studies showed that topical application of insulin could
16
17 accelerate wound healing in diabetes via the activation of insulin signaling pathway,^{32,42} thus the
18
19 sustained release of insulin from the insulin-loaded hydrogel (Figure 4) could facilitate the
20
21 wound healing process. Additionally, live cells (fibroblasts and stem cells) encapsulated in the
22
23 hydrogel can secrete appropriate combinations and ratios of growth factors for enhanced tissue
24
25 regeneration and accelerated wound healing.^{9,43,44} It is reported that fibroblasts play a crucial role
26
27 in the angiogenesis process due to their production of extracellular matrix molecules (e.g.
28
29 collagen I) and their secretion of essential growth factors (e.g. VEGF).^{45,46} These fibroblast-
30
31 derived factors are necessary for endothelial cell sprouting and lumen formation. Research
32
33 displayed that incorporation of fibroblast cells (e.g. human dermal fibroblasts and L929) in
34
35 hydrogels could improve the expression of the growth factors (VEGF) and accelerate wound
36
37 repair.^{19,47} Thus, combining an appropriate dressing material (hydrogel) with drugs and cells
38
39 (such as insulin and L929) could enhance the wound healing process, suggesting the insulin and
40
41 fibroblasts dual-loaded hydrogels as bioactive wound dressings represent an attractive method
42
43 for treating this devastating complication of diabetes.
44
45
46
47
48
49
50
51
52
53
54
55
56
57
58
59
60

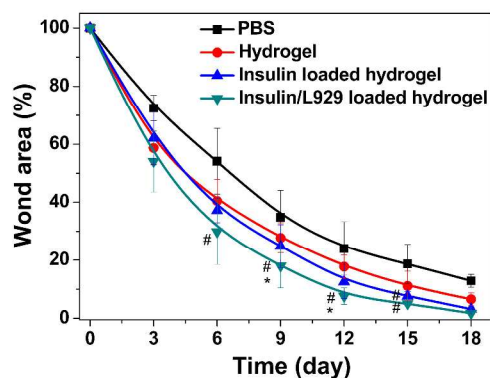
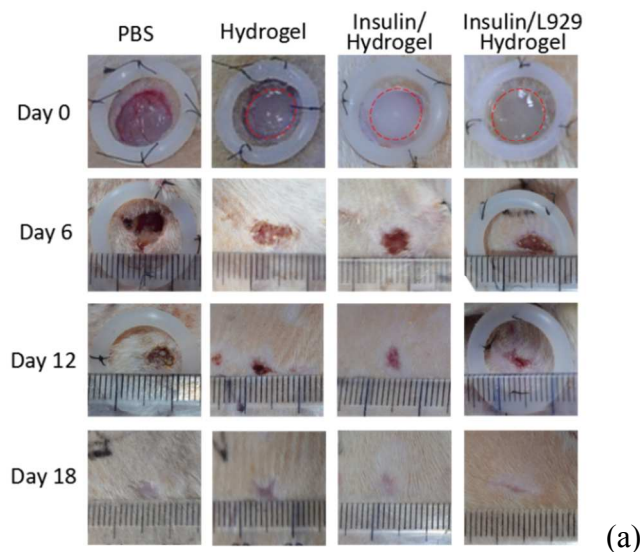


Figure 8. Wound healing by hydrogel dressings in STZ-induced diabetic rats. PBS, hydrogel, insulin-loaded hydrogel, and insulin/L929 loaded hydrogel were administrated on the diabetic skin wound. Representative images of the wound area were taken on day 0, 6, 12, and 18 (a). Wound closure was measured at varied time point using Image J (b). The wound closure was demonstrated as the percentage of wound area at the indicated day compared to the initial wound area. # $p < 0.05$ compared with PBS control group; * $p < 0.05$ compared with hydrogel group.

Inflammatory infiltrate in STZ-induced diabetic wound

1
2
3 Wound healing comprises several overlapping phases: hemostasis, inflammation,
4 proliferation, re-epithelialization and remodeling.⁹ Studies showed that a fibrin plug is formed
5 within hours during hemostasis after injury, and inflammatory cells can be recruited to the
6 wound site due to the cytokines and growth factor released by the aggregated platelets. The
7 aggregation and activation of inflammatory cells are essential for the transition between
8 inflammatory and repair phases.³⁴ H&E staining was performed on day 7 and day 18 after
9 wounding to evaluate inflammatory infiltrate in the wound-healing process. As shown in Figure
10 9a, inflammatory cells with highly condensed chromatin can be observed in all groups at day 7
11 and day 18, and the density of inflammatory cells at day 7 was much higher than that of day 18.
12 Quantitative analysis of the number of mononuclear leucocytes was done by counting the
13 number of cell nuclei per field that had highly condensed chromatin.³³ The results revealed
14 similar inflammatory cell infiltrate in the neat hydrogel group compared with the control group at
15 day 7. A significant increase of inflammatory cell infiltrate in insulin and insulin/L929 hydrogel
16 groups was observed at day 7, which was 1.6-fold higher than that of the control group (Figure
17 9b), possibly due to the topical insulin administration, as reported in previous work.³³ A sharp
18 drop in the number of inflammatory cells in all experimental groups was observed at day 18 as
19 the wound closure, and there was no fester at the wound site during the experimental period.
20 Since some inflammatory cells (e.g. leucocytes) serve as immunologic effectors and sources of
21 growth-promoting cytokines, the infiltration of inflammatory cells in wound areas may be
22 conducive to wound repair.³⁴
23
24
25
26
27
28
29
30
31
32
33
34
35
36
37
38
39
40
41
42
43
44
45
46
47
48
49
50
51
52
53
54
55
56
57
58
59
60

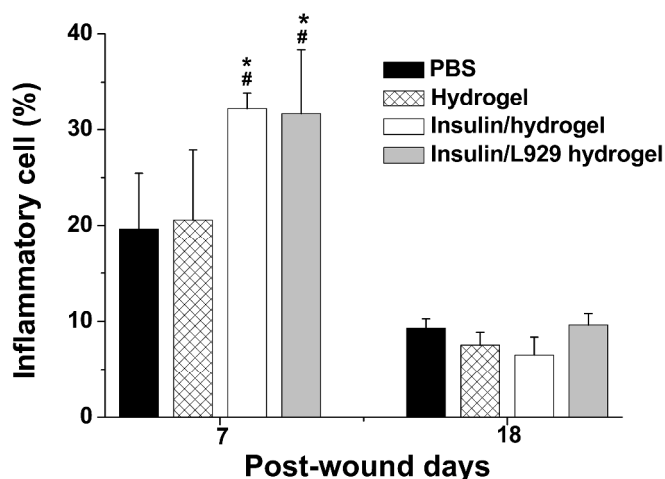
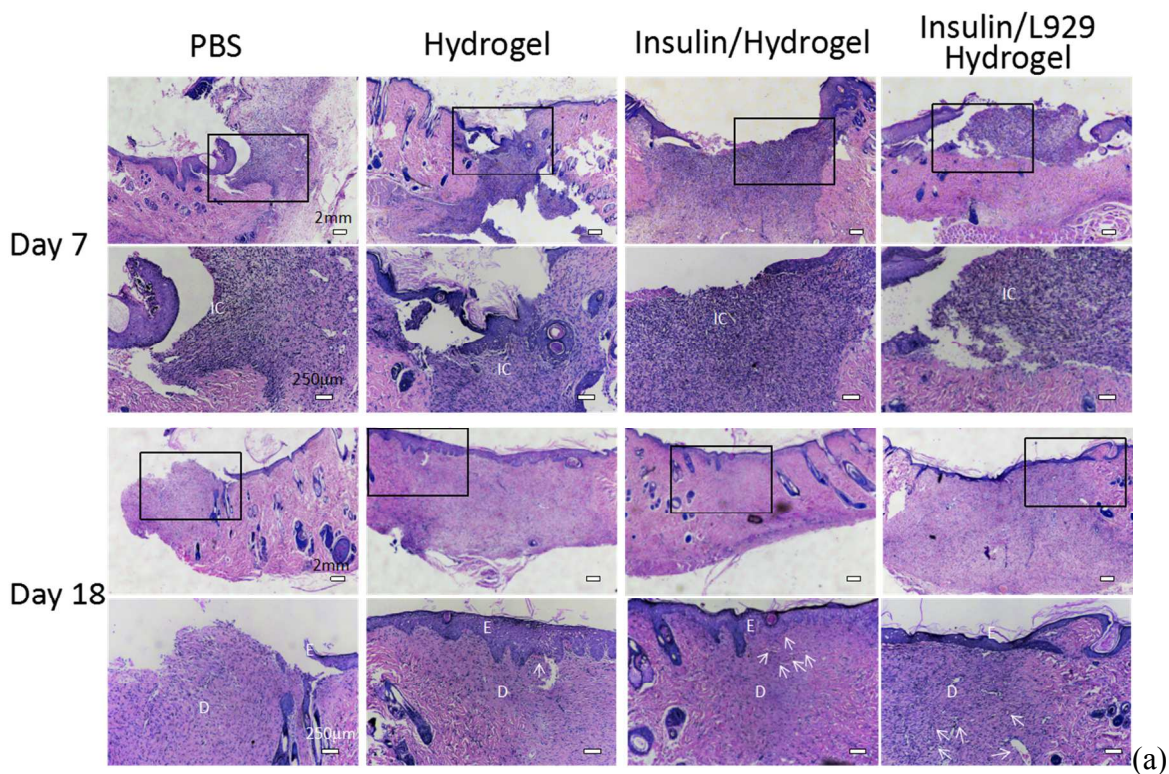


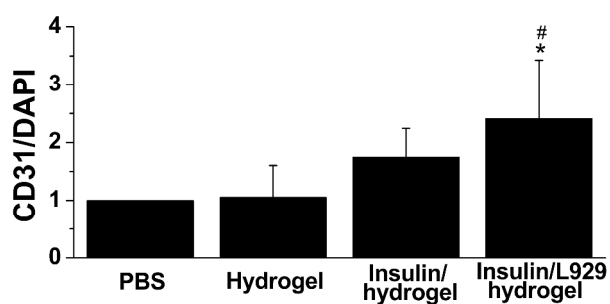
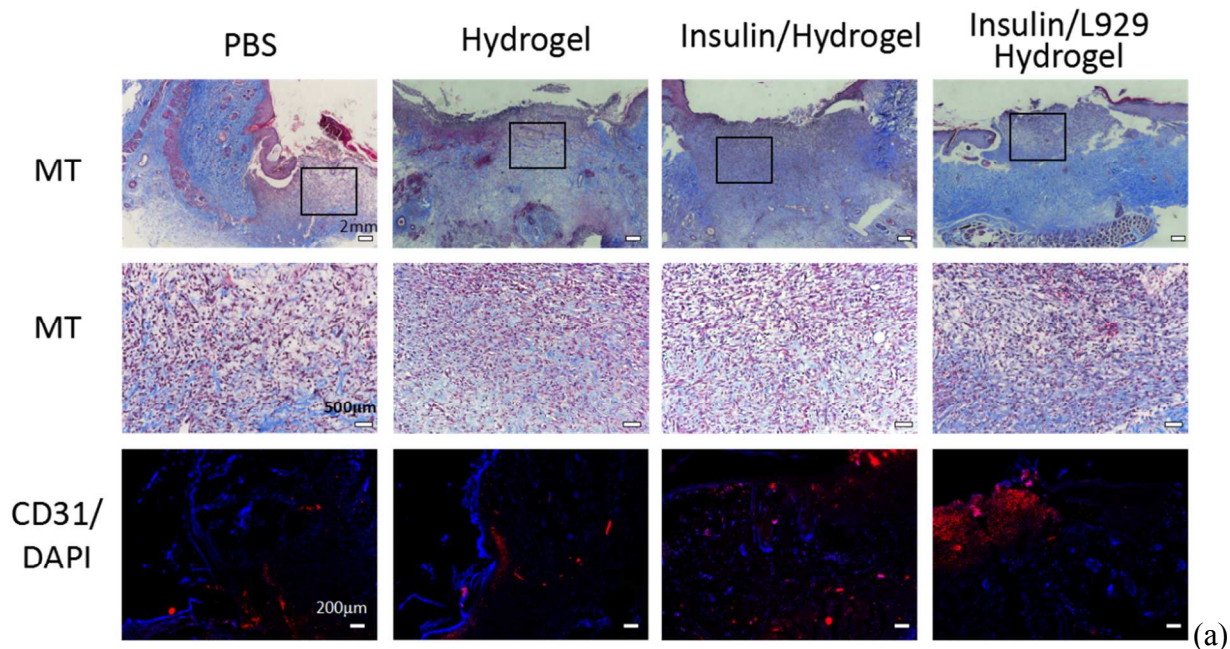
Figure 9 Images of H&E stained histopathological sections after 7 and 18 days of treatment (a). Graphical presentation of the number of inflammatory cells in wound tissue. Quantitative analysis of inflammatory cells was measured using Image J software (b). D, dermis; E, epidermis;

1
2
3 IC, inflammatory cell; Arrows, microvessels. * $p < 0.01$ compared with PBS control group, # $p <$
4
5 0.01 compared with neat hydrogel group.
6
7

8 9 **Neovascularization in STZ-induced diabetic wounds**

10
11
12 Neovascularization is very important in tissue remodeling process. Wounds may fail to heal
13 because of inadequate local vascular supply, for many kinds of substances required for wound
14 repair such as oxygen, nutrients, cells and growth factors are delivered and infiltrated into the
15 wound sites through vasculature during the healing process.⁴⁸ Vascular formation in the wound
16 areas occurs via chemotactic migration of endothelial cells, while this process is suppressed or
17 even not occur in diabetes mellitus.⁴⁹ MT staining and immunocytochemistry were performed to
18 confirm neovascularization in the wound-healing process. As shown in Figure 10, MT staining
19 displayed a few spindle endothelial cells rather than red capillary vasculature in the four
20 experimental groups at day 7. Immunocytochemistry results revealed a remarkably dense
21 population of red CD31-positive cells in the insulin/L929 hydrogel group compared with the
22 control and neat hydrogel groups. Moreover, quantified analysis of the immunochemical results
23 showed a 1.7- and 2.4- fold increased population of CD31-positive cells in the insulin and
24 insulin/L929 hydrogel group respectively, compared with the PBS control group (Figure 10b).
25
26 As a widely known marker of endothelial cells, CD31 positive-cells were considered to
27 contribute to the neovascularization and enhance wound healing.⁵⁰⁻⁵² This was further confirmed
28 by H&E and MT staining carried out on day 18 after wound treatment, and many more red
29 capillary vasculatures were revealed in insulin and insulin/L929 groups than control and neat
30 hydrogel groups (Figure 9a and 11a), being consistent with the immunohistochemistry result. It
31 was reported that topical insulin, growth factors and genes (e.g. VEGF, IL-8 and PDGF-B) used
32 in DFU treatment could enhance neovascularization,^{33, 53-55} thus the insulin and live cells with
33
34
35
36
37
38
39
40
41
42
43
44
45
46
47
48
49
50
51
52
53
54
55
56
57
58
59
60

1
2
3 growth factors secretion encapsulated in the hydrogel dressing as bioactive agents are of great
4
5 importance to neovascularization and wound repair.
6
7
8



46
47 Figure 10. Vascular formation enhanced by insulin/L929 incorporated hydrogel dressings.
48 Immunocytochemical fluorescence reveals CD31-positive cells (red) on day 7 after wounding.
49 Images of MT stained and immunocytochemical sections after 7 days of treatment for the
50 detection of endothelial cells (a), quantification analysis of CD31-positive cells using Image J (b).
51
52
53
54
55
56
57 # $p < 0.05$ compared with PBS control group; * $p < 0.05$ compared with hydrogel group.
58
59
60

Collagen deposition in STZ-induced diabetic wounds

Collagen deposition plays an essential role in the severity of scar formation during the maturation process of wound repair.⁵⁶ MT staining was performed on day 18 after wounding in order to demonstrate the synthesis and accumulation of newly formed collagen in the regenerated skin tissue. The results revealed more collagen deposition on the regenerated tissues in insulin/L929 hydrogel group compared with other groups (Figure 11a). Image J software was used to quantify the collagen deposition in the wound sites by measuring the intensity of the blue areas. As plotted in Figure 11b, wounds of the insulin/L929 hydrogel group displayed $58 \pm 2\%$ of collagen deposition, which was 1.5-fold higher than that of the control group ($40 \pm 1\%$). By comparison, the wounds dealt with neat hydrogel and insulin-loaded hydrogel showed $44 \pm 9\%$ and $52 \pm 10\%$ of collagen deposition, respectively (Figure 11b). At maturation stage of wound healing, wound contraction was resulted due to fibroblasts cross-linked with collagen. It is reported that hyperglycemia impairs wound healing by decreasing cell proliferation and affecting collagen synthesis,³³ hence the enhanced collagen deposition in insulin/L929 loaded hydrogel group may be due to the lower level of blood glucose (Figure 7). In addition, some growth factor (e.g. EFG and bFGF) can increase the accumulation of collagen and keratin so as to reduce scar formation.^{57,58} Thus, the L929 cells may contribute to the effective collagen deposition in insulin/L929 hydrogel group by secreting such growth factors. These findings indicated that combining hydrogel with insulin and live cells promoted neovascularization and collagen deposition and enhanced the wound healing process of diabetic wounds.

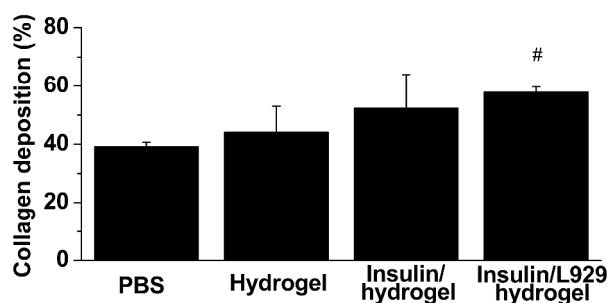
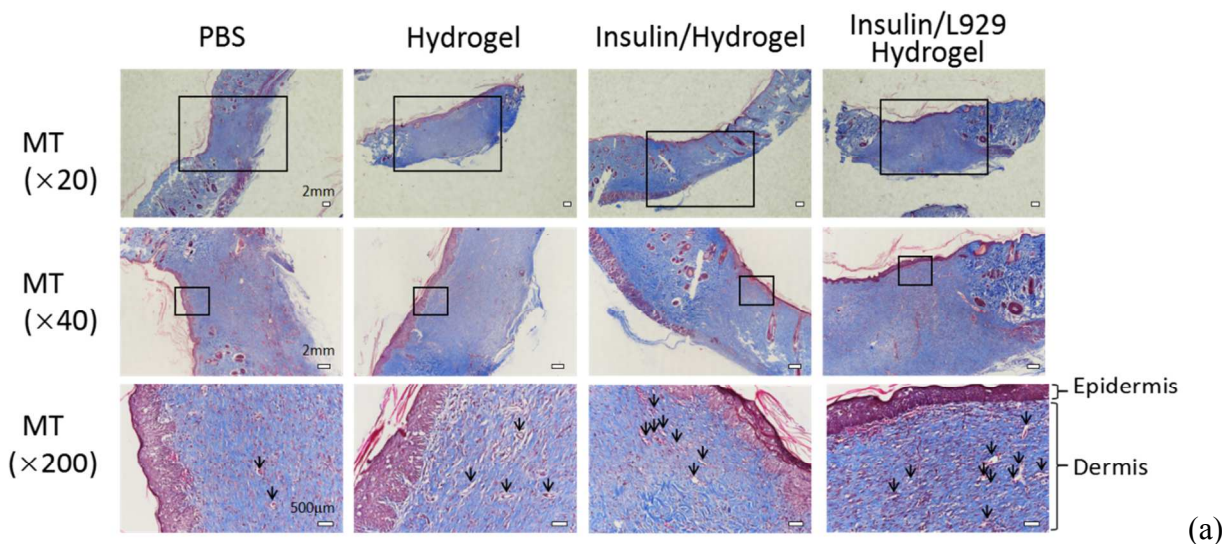


Figure 11. Collagen deposition improved with hydrogels containing insulin and L929 fibroblasts. The tissues of wound sites were performed by MT staining on day 18 after wounding. Blue areas showed newly synthesized collagen fibers and arrows indicate capillary vasculatures (a). The Image J software was used to quantify the collagen deposition in the wound sites (b). [#] $p < 0.05$ compared with PBS control group.

Conclusions

pH and glucose responsive injectable hydrogels were synthesized through the formation of Schiff's base and phenylboronate ester based on phenylboronic modified chitosan (CSPBA),

1
2
3 PVA and OHC-PEG-CHO. Protein drugs and live cells can be encapsulated in the hydrogels
4 during the *in situ* crosslinking process. Sustained and pH/glucose triggered drug release from the
5 hydrogels, and cell viability and proliferation in the three-dimensional hydrogel matrix were
6 observed, allowing the hydrogels to serve as bioactive dressings for diabetic wound repair. *In*
7 *vivo* evaluation of the hydrogel dressings for wound healing was performed using STZ-induced
8 diabetic rat model from general aspects of the wound: the wound closure rate, inflammatory
9 infiltrate, neovascularization, and collagen deposition as well. The results displayed enhanced
10 wound healing of the insulin/L929 hydrogel dressings with increased neovascularization and
11 collagen deposition, suggesting the hydrogels as a delivery platform for various therapeutic
12 proteins and live cells for wound healing applications.
13
14
15
16
17
18
19
20
21
22
23
24
25
26
27

28 ACKNOWLEDGMENT

29
30 This work was financially supported by National Natural Science Foundation of China
31 (51403108, 51773119), K.C. Wong Magna Fund in Ningbo University, Ningbo Municipal
32 Natural Science Foundation (2016A610049), the Science Technology Innovation Commission of
33 Shenzhen Municipality (GJHZ 20160301163644983, JCYJ20170306093157182) and the Health
34 and Family Planning Commission of Shenzhen Municipality (201601019).
35
36
37
38
39
40
41
42

43 **Corresponding Author**

44
45
46 *Lingling Zhao (Email: zhaolingling@nbu.edu.cn), * Hui Tan (E-mail: tanhui@iccas.ac.cn)
47

48 **Author Contributions**

49
50
51 Lingling Zhao and Hui Tan conceived the project. Lingling Zhao and Lijing Niu carried out the
52 preparation and evaluation of the hydrogel dressings. Feiyan Zhu participated in the data
53
54
55
56
57
58
59
60

1
2
3 analysis. Hongze Liang and Chaozong Liu directed the work. Lingling Zhao wrote the initial
4 draft of the manuscript. All authors have given approval to the final version of the manuscript.
5
6
7

8 9 Notes

10 The authors declare no competing financial interest.
11
12

13 REFERENCES

- 14
15
16
17 (1) Shaw, J. E.; Sicree R. A.; Zimmet, P. Z. Global Estimates of the Prevalence of Diabetes for
18 2010 and 2030. *Diabetes Res. Clin. Pract.* **2010**, *87*(1), 4-14.
19
20 (2) Wang, X. L.; Sng, M. K.; Foo, S. L.; Chong, H. C.; Lee, W. L.; Tang, M. B. Y.; Ng, K. W.;
21 Luo, B. W.; Choong, C.; Wong, M. T. C.; Tong, B. M. K.; Chiba, S.; Loo, S. C. J.; Zhu, P. C.;
22 Tan, N. S. Early Controlled Release of Peroxisome Proliferator-Activated Receptor
23 beta/delta Agonist GW501516 Improves Diabetic Wound Healing through Redox
24 Modulation of Wound Microenvironment. *J. Controlled Release* **2015**, *197*, 138-147.
25
26 (3) Moura, L. I. F.; Dias, A. M. A.; Carvalho, E.; de Sousa, H. C. Recent Advances on the
27 Development of Wound Dressings for Diabetic Foot Ulcer Treatment-A Review. *Acta*
28 *Biomater.* **2013**, *9*(7), 7093-7114.
29
30 (4) Alavi, A.; Sibbald, R. G.; Mayer, D.; Goodman, L.; Botros, M.; Armstrong, D. G.; Woo, K.;
31 Boeni, T.; Ayello, E. A.; Kirsner, R. S. Diabetic Foot Ulcers: Part I. Pathophysiology and
32 Prevention. *J. Am. Acad. Dermatol.* **2014**, *70*(1), 1.e1-1.e18.
33
34 (5) Alavi, A.; Sibbald, R. G.; Mayer, D.; Goodman, L.; Botros, M.; Armstrong, D. G.; Woo, K.;
35 Boeni, T.; Ayello, E. A.; Kirsner, R. S. Diabetic Foot Ulcers: Part II. Management. *J. Am.*
36 *Acad. Dermatol.* **2014**, *70*(1), 21.e1-21.e24.
37
38 (6) Da Silva, L.; Carvalho, E.; Cruz, M. T.; Role of Neuropeptides in Skin Inflammation and Its
39 Involvement in Diabetic Wound Healing. *Expert Opin. Biol. Ther.* **2010**, *10*(10), 1427-1439.
40
41 (7) Falanga, V. Wound Healing and Its Impairment in the Diabetic Foot. *Lancet* **2005**,
42 *366*(9498), 1736-1743.
43
44 (8) Game, F. L.; Apelqvist, J.; Attinger, C.; Hartemann, A.; Hinchliffe, R. J.; Löndahl, M.; Price,
45 P. E.; Jeffcoate, W. J.; Int Working Grp Diabet Foot, IWGDF. Effectiveness of Interventions
46 to Enhance Healing of Chronic Ulcers of the Foot in Diabetes: A Systematic Review.
47
48
49
50
51
52
53
54
55
56
57
58
59
60

- 1
2
3
4
5
6
7
8
9
10
11
12
13
14
15
16
17
18
19
20
21
22
23
24
25
26
27
28
29
30
31
32
33
34
35
36
37
38
39
40
41
42
43
44
45
46
47
48
49
50
51
52
53
54
55
56
57
58
59
60
- Diabetes/Metab. Res. Rev.* **2016**, *32*, 154-168.
- (9) Futrega, K.; King, M.; Lott, W. B.; Doran, M. R. Treating the Whole not the Hole: Necessary Coupling of Technologies for Diabetic Foot Ulcer Treatment. *Trends Mol. Med.* **2014**, *20*(3), 137-142.
- (10) Barrientos, S.; Stojadinovic, O.; Golinko, M. S.; Brem, H.; Tomic-Canic, M. Growth Factors and Cytokines in Wound Healing. *Wound Repair Regener.* **2008**, *16*(5), 585-601.
- (11) Park, N. J.; Allen, L.; Driver, V. R. Updating on Understanding and Managing Chronic Wound. *Dermatol. Ther.* **2013**, *26*(3), 236-256.
- (12) Maxson, S.; Lopez, E. A.; Yoo, D.; Danikovitch-Miagkova, A.; Leroux, M. A. Concise Review: Role of Mesenchymal Stem Cells in Wound Repair. *Stem Cells Transl. Med.* **2012**, *1*(2), 142-149.
- (13) Huang, C. C.; Ravindran, S.; Yin, Z. Y.; George, A. 3-D Self-Assembling Leucine Zipper Hydrogel with Tunable Properties for Tissue Engineering. *Biomaterials* **2014**, *35*(20), 5316-5326.
- (14) Lee, K. Y.; Jeong, L.; Kang, Y. O.; Lee, S. J.; Park, W. H. Electrospinning of Polysaccharides for Regenerative Medicine. *Adv. Drug Delivery Rev.* **2009**, *61*(12), 1020-1032.
- (15) Alvarez-Lorenzo, C.; Concheiro, A. Bioinspired Drug Delivery Systems. *Curr. Opin. Biotechnol.* **2013**, *24*(6), 1167-1173.
- (16) Satish, C. S.; Satish, K. P.; Shivakumar, H. G. Hydrogels as Controlled Drug Delivery Systems: Synthesis, Crosslinking, Water and Drug Transport Mechanism. *Indian J. Pharm. Sci.* **2006**, *68*, 133-140.
- (17) Qiu, Y.; Park, K. Environment-Sensitive Hydrogels for Drug Delivery. *Adv. Drug Delivery Rev.* **2001**, *53*(3), 321-339.
- (18) Griffin, D. R.; Weaver, W. M.; Scumpia, P. O.; Di Carlo, D.; Segura, T. Accelerated Wound Healing by Injectable Microporous Gel Scaffolds Assembled from Annealed Building Blocks. *Nat. Mater.* **2015**, *14*(7), 737-744.
- (19) Zhu, F.; Wang, C.; Yang, S.; Wang, Q.; Liang, F.; Liu, C.; Qiu, D.; Qu, X.; Hu, Z.; Yang, Z. Injectable Tissue Adhesive Composite Hydrogel with Fibroblasts for Treating Skin Defects. *J. Mater. Chem. B* **2017**, *5*(13), 2416-2424.
- (20) Yao, Y.; Zhao, L.; Yang, J.; Yang, J. Glucose-Responsive Vehicles Containing Phenylborate Ester for Controlled Insulin Release at Neutral pH. *Biomacromolecules* **2012**, *13*(6), 1837-

- 1
2
3 1844.
4
5 (21) Akbari, A.; Moodi, H.; Ghiasi, F.; Sagheb, H. M.; Rashidi, H., Effects of Vacuum-
6 Compression Therapy on Healing of Diabetic Foot Ulcers: Randomized Controlled Trial. *J.*
7 *Rehabil. Res. Dev.* **2007**, *44* (5), 631-636.
8
9 (22) Chen, F.; Zhu, Y., Chitosan Enclosed Mesoporous Silica Nanoparticles as Drug Nano-
10 Carriers: Sensitive Response to the Barrow pH Range. *Microporous Mesoporous Mater.*
11 **2012**, *150*(1), 83-89.
12
13 (23) Kopeček, J. Hydrogel Biomaterials: A Smart Future? *Biomaterials* **2007**, *28*(34), 5185-5192.
14
15 (24) Zhang, Y.; Tao, L.; Li, S.; Wei, Y. Synthesis of Multiresponsive and Dynamic Chitosan-
16 Based Hydrogels for Controlled Release of Bioactive Molecules. *Biomacromolecules* **2011**,
17 *12*(8), 2894-2901.
18
19 (25) Lin, Y. J.; Lee, G. H.; Chou, C. W.; Chen, Y. P.; Wu, T. H.; Lin, H. R. Stimulation of Wound
20 Healing by PU/Hydrogel Composites Containing Fibroblast Growth Factor-2. *J. Mater.*
21 *Chem. B* **2015**, *3*(9), 1931-1941.
22
23 (26) Yun, E. J.; Yon, B.; Joo, M. K.; Jeong, B. Cell Therapy for Skin Wound Using Fibroblast
24 Encapsulated Poly(ethylene glycol)-poly(L-alanine) Thermogel. *Biomacromolecules* **2012**,
25 *13*(4), 1106-1111.
26
27 (27) Yu, L.; Ding, J. Injectable Hydrogels as Unique Biomedical Materials. *Chem. Soc. Rev.*
28 **2008**, *37*(8), 1473-1481.
29
30 (28) Jeong, B.; Bae, Y. H.; Lee, D. S.; Kim, S. W. Biodegradable Block Copolymers as Injectable
31 Drug-Delivery Systems. *Nature* **1997**, *388*(6645), 860-862.
32
33 (29) Li, J.; Zhang, Y.; Tan, H.; Yan, X.; Zhao, L.; Liang, H. pH and Glucose Dually Responsive
34 Injectable Hydrogel Prepared by In Situ Crosslinking of Phenylboronic Modified Chitosan
35 and Oxidized Dextran. *J. Polym. Sci., Part A: Polym. Chem.* **2015**, *53*(10), 1235-1244.
36
37 (30) Ding, C.; Gu, J.; Qu, X.; Yang, Z. Preparation of Multifunctional Drug Carrier for Tumor-
38 Specific Uptake and Enhanced Intracellular Delivery through the Conjugation of Weak Acid
39 Labile Linker. *Bioconjugate Chem.* **2009**, *20*(6), 1163-1170.
40
41 (31) Ding, C.; Zhao, L.; Liu, F.; Cheng, J.; Gu, J.; Shan-Dan, Liu, C.; Qu, X.; Yang, Z. Dually
42 Responsive Injectable Hydrogel Prepared by In Situ Cross-Linking of Glycol Chitosan and
43 Benzaldehyde-Capped PEO-PPO-PEO. *Biomacromolecules* **2010**, *11*(4), 1043-1051.
44
45 (32) Apikoglu-Rabus, S.; Izzettin, F.V.; Turan, P.; Ercan, F. Effect of Topical Insulin on
46
47
48
49
50
51
52
53
54
55
56
57
58
59
60

- 1
2
3 Cutaneous Wound Healing in Rats with or without Acute Diabetes. *Clin. Exp. Dermatol.*
4 **2010**, 35(2), 180-185.
5
6
7 (33) Azevedo, F.; Pessoa, A.; Moreira, G.; Dos Santos, M.; Liberti, E.; Araujo, E.; Carvalho, C.;
8 Saad, M.; Lima, M. H. Effect of Topical Insulin on Second-Degree Burns in Diabetic Rats.
9 *Biol. Res. Nurs.* **2016**, 18 (2), 181-192.
10
11 (34) Emanuelli, T.; Burgeiro, A.; Carvalho, E. Effects of Insulin on the Skin: Possible Healing
12 Benefits for Diabetic Foot Ulcers. *Arch. Dermatol. Res.* **2016**, 308 (10), 677-694.
13
14 (35) Zhao, L.; Zhu, L.; Wang, Q.; Li, J.; Zhang, C.; Liu, J.; Qu, X.; He, G.; Lu, Y.; Yang, Z.
15 Synthesis of Composite Microgel Capsules by Ultrasonic Spray Combined with In Situ
16 Crosslinking. *Soft Matter* **2011**, 7 (13), 6144-6150.
17
18 (36) Nishi, K. K.; Jayakrishnan, A. Self-Gelling Primaquine-Gum Arabic Conjugate: An
19 Injectable Controlled Delivery System for Primaquine. *Biomacromolecules* **2007**, 8(1), 84-
20 90.
21
22 (37) Zhang, Y.; Yang, B.; Zhang, X.; Xu, L.; Tao, L.; Li, S.; Wei, Y. A Magnetic Self-Healing
23 Hydrogel. *Chem. Commun.* **2012**, 48(74), 9305-9037.
24
25 (38) Roy, D. S.; Rohera, B. D. Comparative Evaluation of Rate of Hydration and Matrix Erosion
26 of HEC and HPC and Study of Drug Release from their Matrices. *Eur. J. Pharm. Sci.* **2002**,
27 16(3), 193-199.
28
29 (39) Jo, S. H.; Ha, K. S.; Moon, K. S.; Kim, J. G.; Oh, C. G.; Kim, Y. C.; Apostolidis, E.; Kwon,
30 Y. I. Molecular Weight Dependent Glucose Lowering Effect of Low Molecular Weight
31 Chitosan Oligosaccharide (GO2KA1) on Postprandial Blood Glucose Level in SD Rats
32 Model. *Int. J. Mol. Sci.* **2013**, 14 (7), 14214-14224.
33
34 (40) Liu, S. H.; Chang, Y. H.; Chiang, M. T. Chitosan Reduces Gluconeogenesis and Increases
35 Glucose Uptake in Skeletal Muscle in Streptozotocin-Induced Diabetic Rats. *J. Agric. Food*
36 *Chem.* **2010**, 58 (9), 5795-5800.
37
38 (41) Ranjbar-Mohammadi, M.; Rabbani, S.; Bahrami, S. H.; Joghataei, M. T.; Moayer, F.
39 Antibacterial Performance and In Vivo Diabetic Wound Healing of Curcumin Loaded Gum
40 Tragacanth/Poly(epsilon-caprolactone) Electrospun Nanofibers. *Mater. Sci. Eng., C* **2016**,
41 69, 1183-1191.
42
43 (42) Lima, M. H. M.; Caricilli, A. M.; de Abreu, L. L.; Araujo, E. P.; Pelegrinelli, F. F.; Thirone,
44 A. C. P.; Tsukumo, D. M.; Pessoa, A. F. M.; dos Santos, M. F.; de Moraes, M. A.;
45
46
47
48
49
50
51
52
53
54
55
56
57
58
59
60

- 1
2
3
4
5
6
7
8
9
10
11
12
13
14
15
16
17
18
19
20
21
22
23
24
25
26
27
28
29
30
31
32
33
34
35
36
37
38
39
40
41
42
43
44
45
46
47
48
49
50
51
52
53
54
55
56
57
58
59
60
- Carvalho, J. B. C.; Velloso, L. A.; Saad, M. J. A. Topical Insulin Accelerates Wound Healing in Diabetes by Enhancing the AKT and ERK Pathways: A Double-Blind Placebo-Controlled Clinical Trial. *PLoS One* **2012**, *7* (5), e36974.
- (43) Shevchenko, R. V.; James, S. L.; James, S. E. A Review of Tissue-Engineered Skin Bioconstructs Available for Skin Reconstruction. *J. R. Soc., Interface* **2010**, *7*(43), 229-258.
- (44) Shi, R.; Jin, Y.; Cao, C.; Han, S.; Shao, X.; Meng, L.; Cheng, J.; Zhang, M.; Zheng, J.; Xu, J.; Li, M. Localization of Human Adipose-Derived Stem Cells and Their Effect in Repair of Diabetic Foot Ulcers in Rats. *Stem Cell Res. Ther.* **2016**, *7*, 155.
- (45) Sorrell, J. M.; Baber, M. A.; Caplan, A. I. A Self-Assembled Fibroblast-Endothelial Cell Co-Culture System that Supports In Vitro Vasculogenesis by Both Human Umbilical Vein Endothelial Cells and Human Dermal Microvascular Endothelial Cells. *Cells Tissues Organs* **2007**, *186* (3), 157-168.
- (46) Newman, A. C.; Nakatsu, M. N.; Chou, W.; Gershon, P. D.; Hughes, C. C. W. The Requirement for Fibroblasts in Angiogenesis: Fibroblast-Derived Matrix Proteins are Essential for Endothelial Cell Lumen Formation. *Mol. Biol. Cell* **2011**, *22* (20), 3791-3800.
- (47) Lee, Y.; Bae, J. W.; Lee, J. W.; Suh, W.; Park, K. D. Enzyme-Catalyzed In Situ Forming Gelatin Hydrogels as Bioactive Wound Dressings: Effects of Fibroblast Delivery on Wound Healing Efficacy. *J. Mater. Chem. B* **2014**, *2*(44), 7712-7718.
- (48) Hoffman, D.; Koch, M.; Krieg, T.; Eming, S. A. Regulation of Angiogenesis: Wound Healing as a Model. *Wound Repair Regener.* **2007**, *15*(6), A138-A138.
- (49) Martin, A.; Komada, M. R.; Sane, D. C. Abnormal Angiogenesis in Diabetes Mellitus. *Med. Res. Rev.* **2003**, *23*(2), 117-145.
- (50) Li, Y.; Zhang, Z.; Kim, H. S.; Han, S.; Kim, S. W. CD31 (+) Cell Transplantation Promotes Recovery from Peripheral Neuropathy. *Mol. Cell. Neurosci.* **2014**, *62*, 60-67.
- (51) Kim, M. H.; Jin, E.; Zhang, H. Z.; Kim, S. W. Robust Angiogenic Properties of Cultured Human Peripheral Blood-Derived CD31 (+) Cells. *Int. J. Cardiol.* **2013**, *166*(3), 709-715.
- (52) Pedrosa, D. C. S.; Tellechea, A.; Moura, L.; Fidalgo-Carvalho, I.; Duarte, J.; Carvalho, E.; Ferreira, L. Improved Survival, Vascular Differentiation and Wound Healing Potential of Stem Cells Co-Cultured with Endothelial Cells. *PLoS One*, **2011**, *6*(1), e16114.
- (53) Yoon, D. S.; Lee, Y.; Ryu, H. A.; Jang, Y.; Lee, K. M.; Choi, Y.; Choi, W. J.; Lee, M.; Park, K. M.; Park, K. D.; Lee, J. W. Cell Recruiting Chemokine-Loaded Sprayable Gelatin

- 1
2
3 Hydrogel Dressings for Diabetic Wound Healing. *Acta Biomater.* **2016**, *38*, 59-68.
4
5 (54) Albrecht-Schgoer, K.; Schgoer, W.; Theurl, M.; Stanzl, U.; Lener, D.; Dejaco, D.; Zelger, B.;
6 Franz, W. M.; Kirchmair, R. Topical Secretoneurin Gene Therapy Accelerates Diabetic
7 Wound Healing by Interaction Between Heparan-Sulfate Proteoglycans and Basic FGF.
8 *Angiogenesis* **2014**, *17*(1), 27-36.
9
10 (55) Keswani, S. G.; Katz, A. B.; Lim, F. Y.; Zoltick, P.; Radu, A.; Alae, D.; Herlyn, M.;
11 Crombleholme, T. M. Adenoviral Mediated Gene Transfer of PDGF-B Enhances Wound
12 Healing in Type I and Type II Diabetic Wounds. *Wound Repair Regener.* **2004**, *12*(5), 497-
13 504.
14
15 (56) Bae, K. H.; Wang, L. S.; Kurisawa, M. Injectable Biodegradable Hydrogels: Progress and
16 Challenges. *J. Mater. Chem. B* **2013**, *1*(40), 5371-5388.
17
18 (57) Choi, J. S.; Choi, S. H.; Yoo, H. S. Coaxial Electrospun Nanofibers for Treatment of
19 Diabetic Ulcers with Binary Release of Multiple Growth Factors. *J. Mater. Chem.* **2011**,
20 *21*(14), 5258-5267.
21
22 (58) Yang, Y.; Xia, T.; Chen, F.; Wei, W.; Liu, C.; He, S.; Li, X. Electrospun Fibers with Plasmid
23 bFGF Polyplex Loadings Promote Skin Wound Healing in Diabetic Rats. *Mol.*
24 *Pharmaceutics* **2012**, *9*(1), 48-58.
25
26
27
28
29
30
31
32
33
34
35
36
37
38
39
40
41
42
43
44
45
46
47
48
49
50
51
52
53
54
55
56
57
58
59
60

Graphic for manuscript

